ANAMET REPORT

ANAMET Report 017
August 1998

Propagation of uncertainty in one-port ANA measurements

P R Young

ANAMET reports are produced by, and for, the members of ANAMET. They are intended for fast dissemination of technical information for discussion purposes and do not necessarily represent an official viewpoint. No responsibility is accepted by the author(s) or ANAMET for any use made of the information contained in this report.

For further information about ANAMET and its activities contact:

internet: **http://www.npl.co.uk/npl/collaboration/clubs/anamet/index.html**

e-mail: **anamet@npl.co.uk**

Comments on this report should be sent to:

mail: **ANAMET**
Building 72
National Physical Laboratory
Queens Road
Teddington
Middlesex
TW11 0LW

fax: **0181 943 6037 (UK)**
+44 181 943 6037 (elsewhere)

This report has been approved by the ANAMET Steering Committee.

PROPAGATION OF UNCERTAINTY IN ONE-PORT ANA MEASUREMENTS

P. R. Young
Centre for Electromagnetic Metrology
National Physical Laboratory

1 Introduction

Many factors affect the accuracy of a reflection coefficient measurement. Connector repeatability, noise, non-linearity in the mixers, errors in the ADCs are just some of the many sources of uncertainty in a modern network analyser system. There is, however, a more fundamental, and often overlooked, contribution to the overall uncertainty in an ANA measurement. Namely the imperfections of the standards used in calibration. Since these standards are used to characterise the internal network of the test set, any deviation between the assumed and actual values of the standards will introduce an error in both the calibration and subsequent measurement of a device under test (DUT). Fortunately, we can relate the uncertainty in the measurement to that of the assumed values of the calibration standards. This report demonstrates such a technique for a simple one-port ANA. Note that a brief account of this technique was covered in a recent ANAMET news article [1].

2 Theory

It is well known that the true value ρ of the voltage reflection coefficient (VRC) for a device connected to a reflectometer is related to the indicated value w by

$$w = E_{DF} + \frac{E_{RF}\rho}{1 - E_{SF}\rho} \tag{1}$$

where E_{DF}, E_{SF} and E_{RF} are the familiar directivity, source match and frequency tracking terms, respectively. It is more convenient to write equation (1) as a bilinear equation [2, 3]:

$$w = \frac{A\rho + B}{C\rho + 1} \tag{2}$$

where A, B and C are related to E_{DF}, E_{SF} and E_{RF}. In practice, A, B and C are not known, but are determined in calibration. By connecting three standards to the reflectometer, a system of linear equations is obtained, which can be solved for A, B and C. Thus,

$$w_i = \frac{A\rho_i + B}{C\rho_i + 1} \qquad i = 1, 2, 3. \tag{3}$$

The reflection coefficient for an unknown DUT is then given by

$$\rho = \frac{B - w}{Cw - A}. \tag{4}$$

In practice, the VRCs of the standards ρ_i are not known exactly; only approximate values based on theoretical models, prior measurements or engineering assumptions are available. Therefore, the relationship between the indicated values and the assumed values is given by

$$w_i = \frac{A'\Gamma_i + B'}{C'\Gamma_i + 1}, \qquad i = 1, 2, 3. \tag{5}$$

where w_i and Γ_i are the indicated and assumed values of the ith standard, respectively. We note that for three given standards the values of w_i are identical in the equations (3) and (5). However, since $\Gamma_i \neq \rho_i$:

$$A \neq A',\ B \neq B' \text{ and } C \neq C'.$$

For an unknown DUT, equation (5) becomes

$$\Gamma = \frac{B' - w}{C'w - A'} \tag{6}$$

where, Γ is the corrected value of the DUT. We note that for a given DUT, w is identical in equations (4) and (6).

Suppose that the difference between the assumed and true values of the standards is small (which should be the case for precision items), and that this difference is represented by ε_i. Thus,

$$\Gamma_i = \rho_i + \varepsilon_i \tag{7}$$

We require the difference between the true value of the DUT and the corrected value, calculated from equation (6),

$$\Delta = \Gamma - \rho.$$

To derive a relationship between the true and assumed values we first eliminate the calibration constants from equation (3) and (4). This is achieved by using the property that the cross ratio of four complex numbers is invariant under a bilinear transform [4]. Thus equations (3) and (4) can be written as

$$\frac{(w - w_1)(w_2 - w_3)}{(w - w_3)(w_2 - w_1)} = \frac{(\rho - \rho_1)(\rho_2 - \rho_3)}{(\rho - \rho_3)(\rho_2 - \rho_1)} \tag{8}$$

Where now the constants A, B and C have been eliminated. We note that ρ and w are the true and indicated values of the DUT, respectively. Similarly, equations (5) and (6) can be written as

$$\frac{(w - w_1)(w_2 - w_3)}{(w - w_3)(w_2 - w_1)} = \frac{(\Gamma - \Gamma_1)(\Gamma_2 - \Gamma_3)}{(\Gamma - \Gamma_3)(\Gamma_2 - \Gamma_1)} \tag{9}$$

where Γ and w are the corrected and indicated values for the same DUT, respectively. Therefore, for three calibration standards with true values ρ_i, assumed values Γ_i and indicated values w_i, the following expression relates the true value of the measurand ρ to that of the corrected value Γ.

$$\frac{(\rho-\rho_1)(\rho_2-\rho_3)}{(\rho-\rho_3)(\rho_2-\rho_1)} = \frac{(\Gamma-\Gamma_1)(\Gamma_2-\Gamma_3)}{(\Gamma-\Gamma_3)(\Gamma_2-\Gamma_1)} \tag{10}$$

Eliminating ρ_i from equations (7) and (10) and noting that Δ is small [5] gives

$$\Delta(\rho) = \Gamma - \rho = \varepsilon_1 a_1(\rho) + \varepsilon_2 a_2(\rho) + \varepsilon_3 a_3(\rho) \tag{11}$$

with

$$a_1(\rho) = \frac{(\rho-\Gamma_2)(\rho-\Gamma_3)}{(\Gamma_1-\Gamma_2)(\Gamma_1-\Gamma_3)}, \tag{11a}$$

$$a_2(\rho) = \frac{(\rho-\Gamma_3)(\rho-\Gamma_1)}{(\Gamma_2-\Gamma_3)(\Gamma_2-\Gamma_1)} \tag{11b}$$

and

$$a_3(\rho) = \frac{(\rho-\Gamma_1)(\rho-\Gamma_2)}{(\Gamma_3-\Gamma_1)(\Gamma_3-\Gamma_2)}; \tag{11c}$$

where second order terms have been neglected. We now have an expression relating the difference between the true and corrected value of the DUT to the difference between the true and assumed values of the standards.

If instead of difference terms, we replace ε_i with circles of uncertainty of radii u_i centred around Γ_i (so that ρ_i is somewhere on, or within, the circle), then the uncertainty in the measurement is given by [1]

$$U(\rho) = u_1|a_1(\rho)| + u_2|a_2(\rho)| + u_3|a_3(\rho)| \tag{12}$$

By plotting $U(\rho)$ for complex ρ, we obtain surface plots, or *uncertainty profiles*, indicating the uncertainty in the measured DUT for a given ρ.

3 Uncertainty profiles

This section shows uncertainty profiles for three different calibration schemes: calibration using offset high-reflect standards and short-open-load calibrations using the GPC-7 and Type-N connector types. It is clear from (12) that the uncertainty in the measured DUT is dependent on the assumed values of the standards and their uncertainties. Since both the assumed values and their associated uncertainties are likely to be functions of the operating frequency, $U(\rho)$ will also be frequency dependent.

In practice, the uncertainties of the three calibration standards are different. For example a short-circuit is likely to better defined than a nominal 50 Ω load. However, to simplify the analysis, we will assume that the uncertainties are equal, $u = u_1 = u_2 = u_3$.

In each of the following figures the uncertainty is indicated by the height and colour of the surface, the value being given from the colour bars to the right of the plots. A contour of the surface is also provided. The red circles on the contour plots denote the assumed positions of the calibration standards at the relevant frequency. The plots show relative uncertainty $U(\rho)/u$, i.e., the factor by which the uncertainty in the DUT is greater than that of the calibration standards, at a given point in the complex plane.

3.1 Offset high-reflect calibration

Figure 1 shows uncertainty profiles for an offset high-reflect calibration with short-circuits offset by 0 mm, 150 mm and 300 mm. Figure 1(a) through to Figure 1(e) show the calibration at frequencies in steps of 60 MHz, starting at 150 MHz and ending at 450 MHz. The assumed values for the standards are given by

Flush Short-circuit: $\Gamma_1 = -1$

Short-circuit offset by 150 mm: $\Gamma_2(f) = -\exp(-j\beta 2L_1)$

Short-circuit offset by 300 mm: $\Gamma_3(f) = -\exp(-j\beta 2L_2)$

where $\beta = 2\pi f / v$ is the propagation constant of the line, v is the phase velocity of the propagating mode and $L_1 = 150$ mm and $L_2 = 300$ mm are the lengths of the two lines.

We observe from Figure 1 that the uncertainty in the measurement varies quite dramatically over the complex plane. Furthermore, there is a strong frequency dependence. In Figure 1(a) the refection coefficient of the three standards are close together resulting in large uncertainties at points away from the calibration standards. As the frequency increases, both the offset short-circuits rotate clockwise around the edge of the unit circle resulting in more uniform profiles, figures 1(b) and 1(c). In Figure 1(d) the standards are separated by 120°. We see that now the uncertainty is almost uniform at the centre of the complex plane, rising to $1.7u$ on the circumference of the unit circle at points 60° away from the standards. Under these operating conditions the calibration is at its optimum. Whereby optimum we mean, low, uniform uncertainty.

As the frequency increases past the optimum point, the VRC of the short-circuit offset by 300 mm moves closer to the flush short-circuit (Figure 1(e)) resulting in increased uncertainty. Finally, in Figure 1(f), we obtain a saddle-shaped uncertainty profile, which is low, close to the standards, but increases towards the origin and at points on the circumference, away from the standards. This trend continues for further increases in frequency until Γ_3 passes through -1. At this point, there are effectively only two values for Γ_i and therefore the system of equations in (3) and (6) become indeterminate. Under these conditions, equation (12) is meaningless. We note, that in practice, additional offset high-reflect standards could be used for broadband calibrations. Then, at a given frequency, standards that result in uncertainty profiles closest to the optimum condition could be chosen.

(a) 150 MHz

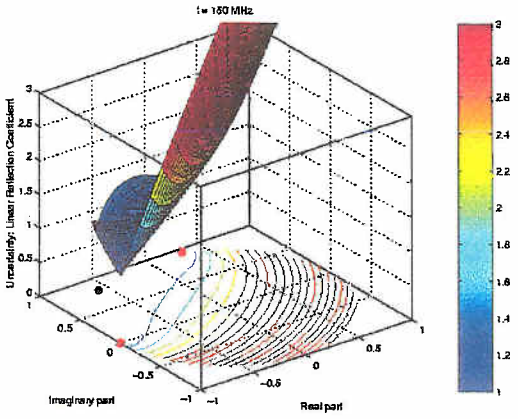

(b) 210 MHz

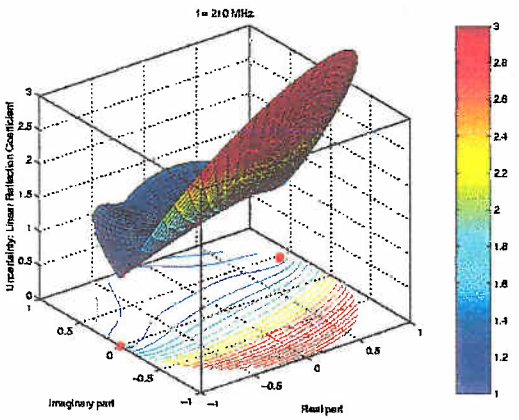

(c) 270 MHz

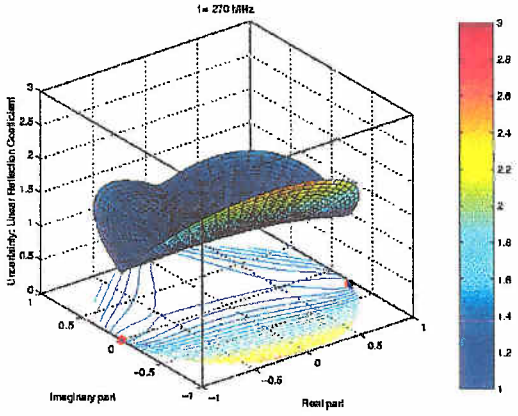

(d) 330 MHz

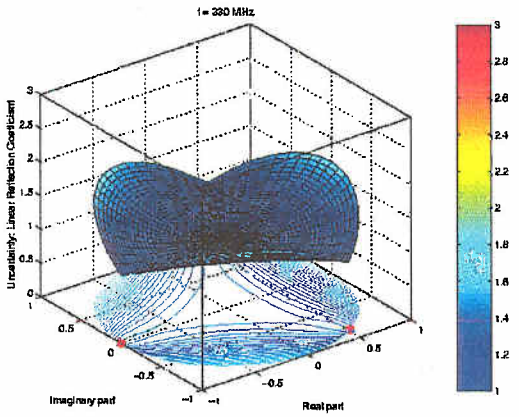

(e) 390 MHz

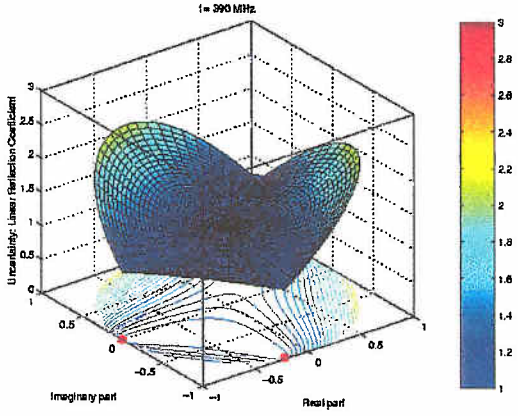

(f) 450 MHz

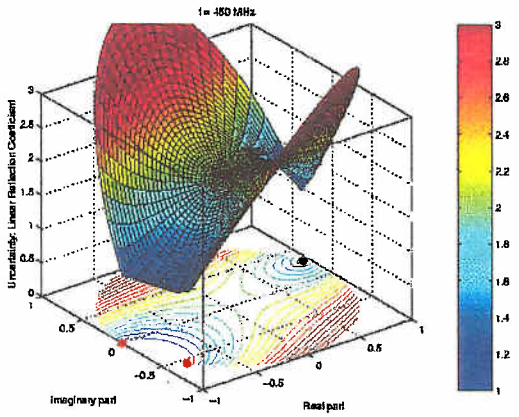

Figure 1. Relative uncertainty in the measurement, $U(\rho)/u$, for an offset short-circuit calibration as a function of the true value of the DUT, ρ. The uncertainty is indicated by the height and colour of the surface. The red circles denote the positions of the calibration standards at the relevant frequency.

3.2 GPC-7 short-open-load calibration

Figure 2 shows uncertainty profiles for a GPC-7 short-open-load calibration for frequencies up to 18 GHz. In each case the open-circuit has been modelled as a capacitor with the following frequency dependence [6]

$$C(f) = c_0 + c_1 f + c_2 f^2 + c_3 f^3$$

where

$$c_0 = 87.2 \times 10^{-15} \text{ F},$$
$$c_1 = 1695 \times 10^{-27} \text{ F s},$$
$$c_2 = -150.5 \times 10^{-36} \text{ F s}^2$$

and

$$c_3 = 8.89 \times 10^{-45} \text{ F s}^3.$$

The assumed values of the standards are

Short-circuit: $\Gamma_1 = -1$

Matched load: $\Gamma_2 = 0$

Open-circuit with fringing capacitance: $\Gamma_3(f) = \dfrac{1 - j\omega C(f) Z_0}{1 + j\omega C(f) Z_0}$

where $\omega = 2\pi f$ is the angular frequency and Z_0 is the characteristic impedance of the line.

Figure 2(a) shows the GPC-7 calibration at DC. Here the uncertainty profile resembles a butterfly, with low uncertainty along the real axis rising to a maximum at $\pm j$. As the frequency increases, the reflection coefficient of the open-circuit rotates clockwise around the circumference of the unit circle. This results in an increased uncertainty in the upper half of the complex domain with a corresponding decrease in the lower half. This trend continues for further increases in frequency until the upper frequency limit of the GPC-7 connector type is reached at $f = 18$ GHz.

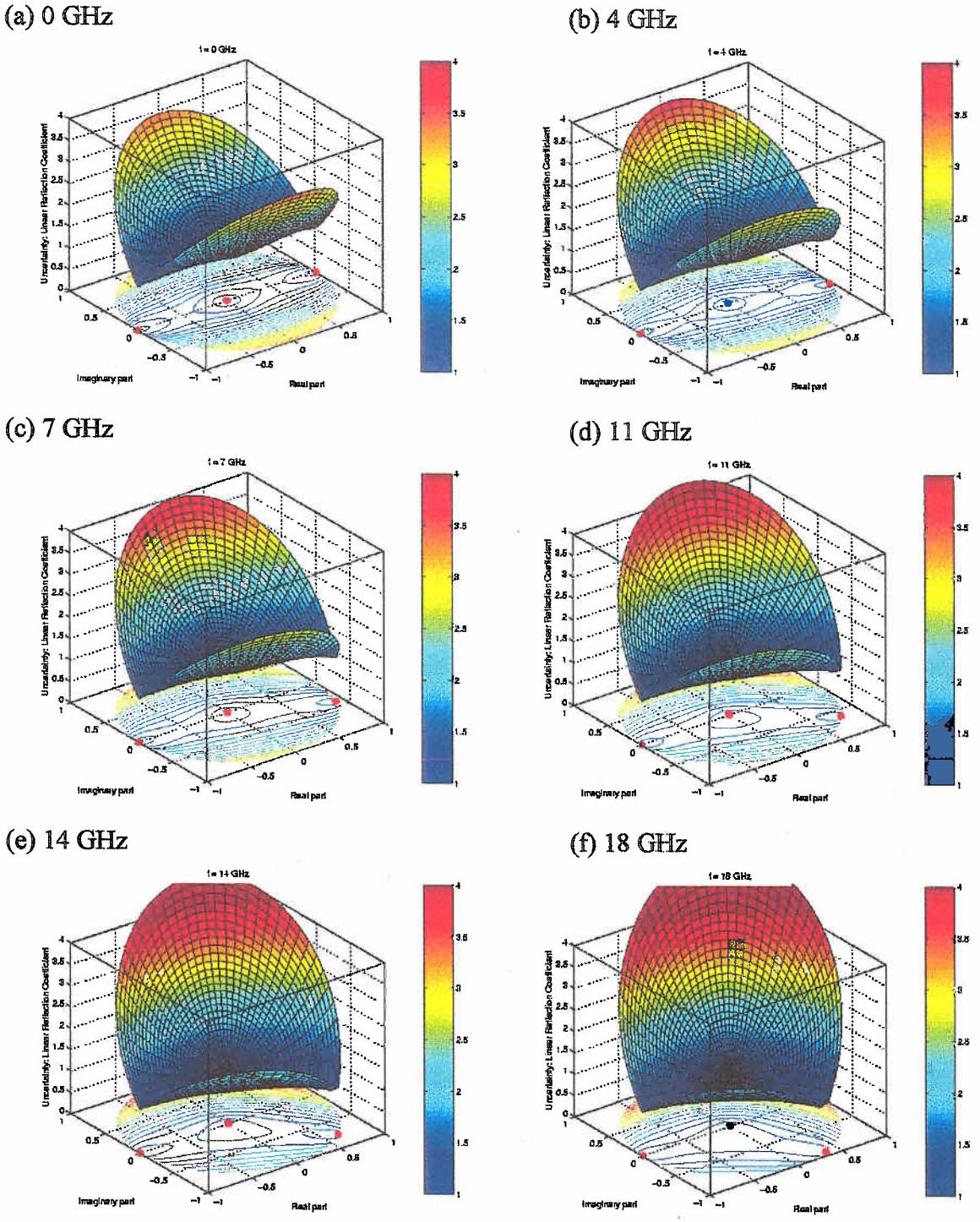

Figure 2. Relative uncertainty in the measurement, $U(\rho)/u$, for a GPC-7 short-open-load calibration as a function of the true value of the DUT, ρ. The uncertainty is indicated by the height and colour of the surface. The red circles denote the positions of the calibration standards at the relevant frequency.

3.3 Type-N short-open-load calibration

Figure 3 shows uncertainty profiles for a Type-N short-open-load calibration. In this case, the open-circuit and short-circuit include an offset of 6.9 mm and 8.4 mm, respectively. Again the open-circuit is modelled as a capacitor with the following frequency characteristics [7]

$$C(f) = c_0 + c_1 f + c_2 f^2 + c_3 f^3$$

where

$$c_0 = 88.308 \times 10^{-15} \text{ F},$$

$$c_1 = 1667.2 \times 10^{-27} \text{ F s},$$

$$c_2 = -146.61 \times 10^{-36} \text{ F s}^2$$

and

$$c_3 = 9.7531 \times 10^{-45} \text{ F s}^3.$$

The assumed values are

Short-circuit: $\Gamma_1 = -1$

Short-circuit offset by 8.4 mm: $\Gamma_2(f) = -\exp(-j\beta 2 L_1)$

Open-circuit offset by 6.9 mm: $\Gamma_3(f) = \dfrac{1 - j\omega C(f) Z_0}{1 + j\omega C(f) Z_0} \exp(-j\beta 2 L_2)$

where $L_1 = 8.4$ mm and $L_2 = 6.9$ mm are the lengths of the line sections within the short-circuit and open-circuit, respectively.

At DC the Type-N calibration is identical to the GPC-7 calibration. However, as the frequency increases, the VRC of both the open-circuit and the short-circuit rotate clockwise around the circumference of the unit circle, at approximately the same rate (with this trend continuing above 10 GHz). As a result, the uncertainty profile rotates around the origin, retaining its original butterfly shape. Therefore, for the Type-N calibration, the standards always retain their relative position in the complex plane.

(a) 0 GHz

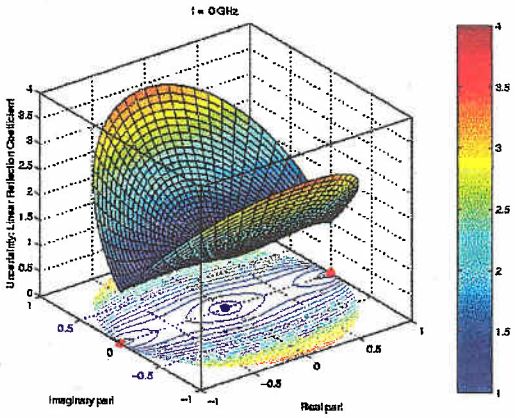

(b) 2 GHz

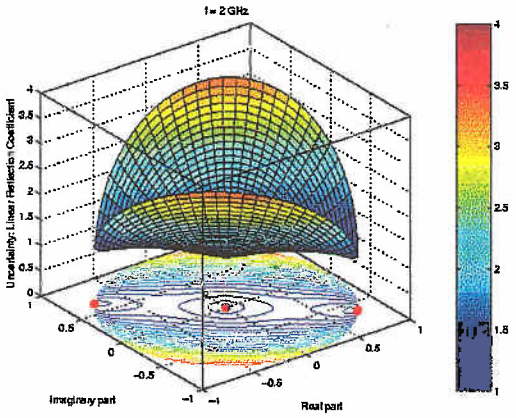

(c) 4 GHz

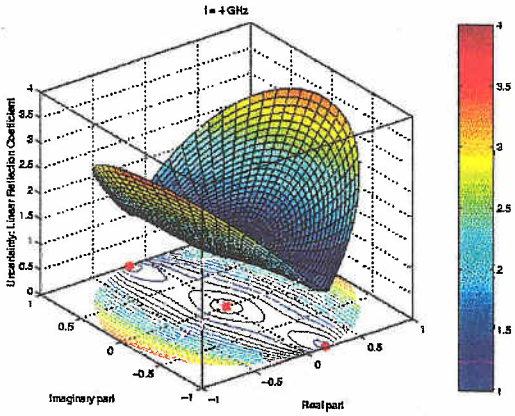

(d) 6 GHz

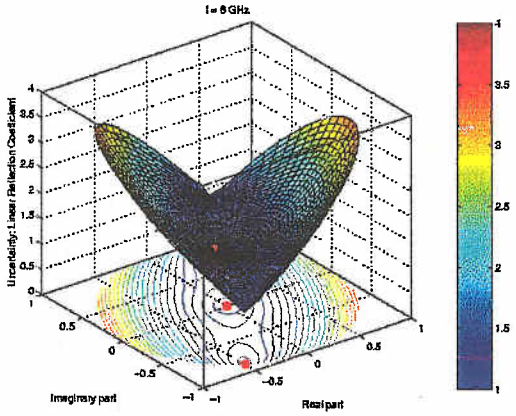

(e) 8 GHz

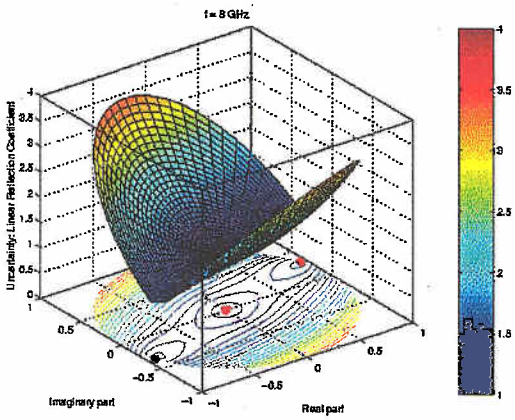

(f) 10 GHz

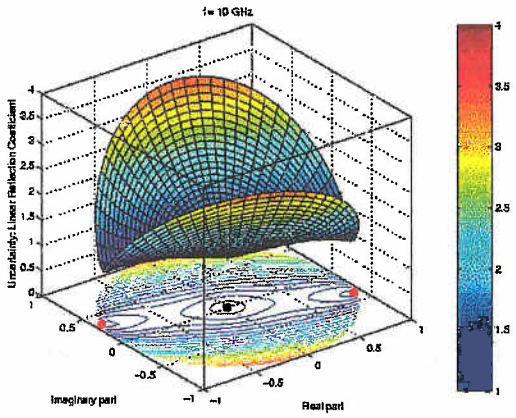

Figure 3. Relative uncertainty in the measurement, $U(\rho)/u$, for a Type-N short-open-load calibration as a function of the true value of the DUT, ρ. The uncertainty is indicated by the height and colour of the surface. The red circles denote the positions of the calibration standards at the relevant frequency.

Conclusions

It has been shown that the uncertainty in an ANA reflection measurement can be related to the assumed values of the standards used to calibrate the ANA, their uncertainty and the true value of the DUT. Since the assumed values of the standards and their associated uncertainty are in general functions of frequency the uncertainty in measurement is also frequency dependent. This results in a complicated, but predictable, relationship between the uncertainty in the measurement and the uncertainty in the assumed values of the standards.

Three typical calibrations were considered in this report; however the technique is applicable to any one-port calibration. It was shown that an offset short-circuit calibration exhibits low, uniform, uncertainty profiles when operating under its optimal conditions. Unfortunately, the calibration is very sensitive to frequency, displaying large uncertainties for relatively small changes in frequency. In contrast the GPC-7 calibration was shown to have very little frequency dependence, with little change in the uncertainty profile over the recommended operating range. The Type-N calibration proved to be quite frequency dependent but stable for all operating frequencies.

It is clear, then, that the uncertainty in the assumed values of the standards should not, as is often the case, be neglected. In fact, under certain conditions, it could well be the dominant contribution to the overall uncertainty.

Acknowledgements

The work described in this report was supported by the UK's Department of Trade and Industry's National Measurement System Policy Unit.

References

1 P. R. Young, "Predicting uncertainties in ANA calibrations," *ANAMET news*, Issue 10, pp. 5-8, Spring 1998.

2 G. F. Engen, "Microwave circuit theory and foundations of microwave metrology," Peter Peregrinus Ltd., London, 1992.

3 P. I. Somlo and J. D. Hunter, "Microwave impedance measurement," Peter Peregrinus Ltd., London, 1985.

4 R. V. Churchill, J. W. Brown and R. F. Verhey, "Complex variables and applications," third edition, McGraw-Hill book company, 1976.

5 B. Bianco, A. Corana, S. Ridella and C. Simicich, "Evaluation of errors in calibration procedures for measurements of reflection coefficient," *IEEE Trans. Instrum. Meas.*, vol. IM-27, no 4, pp. 354-358, December 1978.

6 Hewlett Packard, 7 mm precision calibration kit, 85050C, cal. definitions disk.

7 Hewlett Packard, Type N calibration kit, 85054B, cal. definitions disk.